Predicting and Reducing Liquation-Cracking Susceptibility Based on Temperature vs. Fraction Solid

Elimination of cracking from welds of highly crack-susceptible aluminum alloys is demonstrated

BY G. CAO AND S. KOU

ABSTRACT. Aluminum welds are susceptible to liquation cracking in the partially melted zone (PMZ). This is the region immediately outside the fusion zone where liquation occurs due to overheating during welding. Using the multicomponent Scheil model for alloy solidification, curves of temperature vs. fraction solid (T-f_S) during solidification were calculated for the PMZ and weld metals (WMs) made with filler metals of various compositions. These curves were used to predict the crack susceptibility by checking whether the harmful condition of WM f_S > PMZ f_S exists during PMZ solidification, then reduce the susceptibility by minimizing this condition. This approach was tested against complete joint penetration welds of Alloys 7075 and 2024, which are highly susceptible to liquation cracking. In the case of 7075, T-f_S curves predicted: 1) crack susceptibility of welds made with filler metals 4043, 4047, and 4145 and 2) crack elimination through 4145 plus extra Cu. Both predictions were confirmed in circular-patch welding. Similarly, in the case of 2024, T-f_S curves predicted both the crack susceptibility with filler metals 1100 and 4043 and crack elimination through 5356 plus extra Cu, and both predictions were confirmed. This approach can be used to guide the selection or development of filler metals that reduce the crack susceptibility.

Introduction

The partially melted zone (PMZ) is the region immediately outside the fusion zone where liquation occurs during welding because of heating above the eutectic temperature (or the solidus temperature if the workpiece is completely solutionized before welding) (Ref. 1). Liquation can occur along the grain boundary as well as in the grain interior. Cracking can occur along the grain boundary under tensile strains that are induced in the workpiece, which is restrained and thus unable to contract freely upon cooling during welding. Aluminum alloys are known to be susceptible to liquation cracking in the PMZ during welding (Refs. 1–23).

Metzger (Ref. 3) observed liquation cracking in complete joint penetration GTA (gas tungsten arc) welds of Alloy 6061 made with Al-Mg fillers at high dilution ratios, but not in similar welds made with Al-Si fillers at any dilution ratios. This was confirmed by subsequent studies on 6061 and similar alloys such as 6063 and 6082 (Refs. 5, 7–12). Gittos and Scott (Ref. 5) used the circular-patch test (Ref. 24) to study liquation cracking in an aluminum alloy close to Alloy 6082 in composition. Liquation cracking occurred in complete joint penetration GTA welds made with an essentially Al-5Mg filler at high dilution ratios (about 80%), but not with an essentially Al-5Si filler at any dilution ratios. They proposed that liquation cracking occurs when the base metal solidus temperature is below the weld metal solidus temperature. Gutscher and Cross (Ref. 16) studied the effect of Cu and Fe contents on the solidification cracking and liquation in Alloy 2519.

Katoh et al. (Ref. 7), Kerr et al. (Ref. 8), and Miyazaki et al. (Ref. 9) used the Varestraint test to study liquation cracking in partial joint penetration GTA and GMA welds of 6000 alloys. Their results contradicted the cracking condition of Gittos and Scott (Ref. 5). Huang and Kou (Refs. 19, 22) studied liquation cracking in partial joint penetration welds of aluminum alloys. The papillary (nipple) type penetration common in GMAW with Ar shielding, where metal transfer is by the spray mode, was found to oscillate along the weld and cause cracking (Ref. 19). A new mechanism was proposed to explain such liquation cracking.

Recently, Kou and his coworkers (Refs. 20, 21, 23) studied liquation cracking in complete joint penetration aluminum welds using circular-patch testing, then analyzed their results with the curves of temperature (T) vs. fraction solid (f_S) of the weld metal (WM) and the PMZ. It was found that WM f_S > PMZ f_S existed throughout PMZ solidification of the Al-Cu welds that liquation cracked (Ref. 20), during PMZ terminal solidification in the Al-Mg-Cu welds that liquation cracked (Ref. 21), and after f_S exceeded about 0.3 in the Al-Si welds that liquation cracked (Ref. 23). Thus, it can be concluded from these three studies that a weld is susceptible to liquation cracking if WM f_S > PMZ f_S exists after the PMZ has developed some strength, say, after f_S reaches about 0.3. This value of 0.3 will be explained subsequently in Section 3 of Results and Discussion. It should be mentioned that the mechanism of liquation cracking in partial joint penetration aluminum welds can involve the dynamics of penetration oscillation (Ref. 19) and, consequently, this conclusion may not apply.

In the present study, WM and PMZ T-f_S curves of welds of Alloys 7075 and 2024, which are highly susceptible to liquation and liquation cracking, are calculated based on the multicomponent Scheil model to predict and reduce their liquation cracking susceptibility. The results are verified using circular-patch welding.

KEYWORDS

Liquation Cracking
Partially Melted Zone (PMZ)
Temperature vs. Fraction Solid (T-f_S)
Weld Metals (WMs)
Circular-patch Test
Circular-patch Welding

Experimental Procedure

The circular-patch test (Ref. 24) was used to evaluate the susceptibility to liquation cracking, as shown in Fig. 1. In order to prevent the workpiece from contracting freely during welding, the workpiece was

G. CAO is a graduate student and S. KOU (skou@wisc.edu) *is a professor in the Department of Materials Science and Engineering, University of Wisconsin, Madison, Wis.*

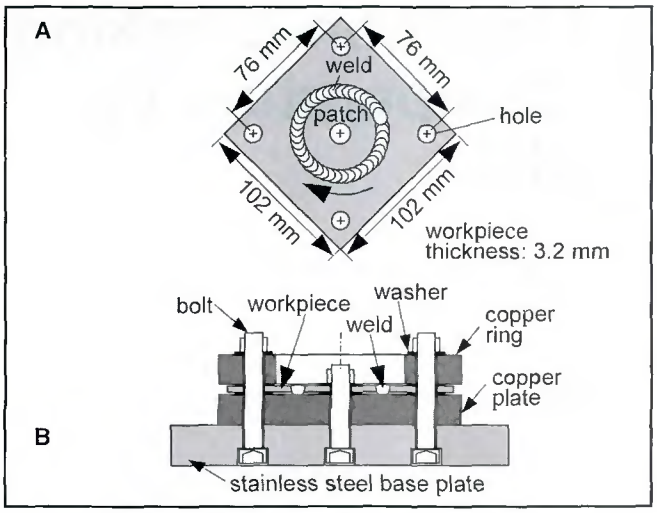

Fig. 1 — Circular-patch welding. A — Top view of workpiece; B — side view of apparatus.

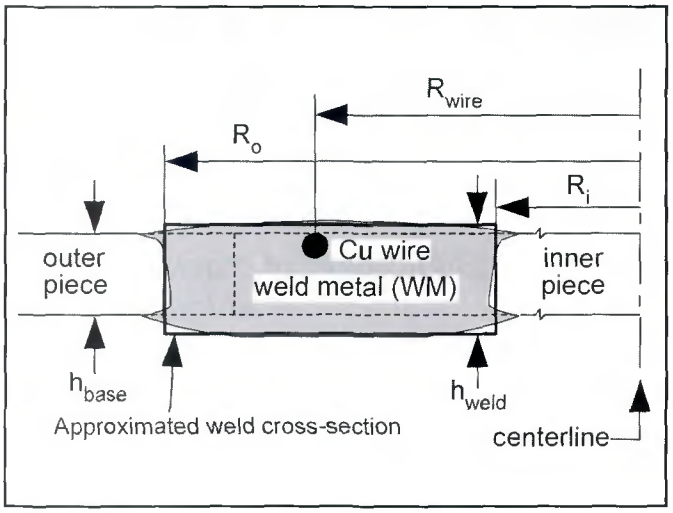

Fig. 2 — Approximated weld transverse cross section.

Table 1 — Compositions of Materials in wt-%

	Cu	Mn	Mg	Cr	Zn	Ti	Si	Fe
			Workpiece					
2024	4.60	0.63	1.50	—	0.12	0.03	0.06	0.17
7075	1.45	0.05	2.59	—	5.8	—	0.08	—
			Filler Metals					
1100	0.08	0.01	—	—	0.02	—	0.08	0.52
4043	—	—	—	—	—	—	5.25	—
4047	0.03	—	0.02	—	—	—	11.6	—
4145	3.9	0.01	0.05	—	0.03	—	9.9	—
5356	0.10	0.05	5.00	0.05	0.10	0.06	0.25	0.40

highly restrained by being bolted down to a thick stainless steel plate. The workpiece, as shown in Fig. 1A, consisted of an outer piece and an inner piece (the circular patch) of the same metal. Alloy 7075 was welded in the as-received T6 condition, and Alloy 2024 in the as-received T3 condition (Ref. 25). Several filler metals were used, including 1100 (essentially pure Al), 4043 (essentially Al-5Si), 4047 (essentially Al-12Si), 5356 (essentially Al-5Mg), and 4145 (essentially Al-4Cu-10Si). The actual compositions of all alloys are listed in Table 1.

The outer piece was 102 × 102 × 3.2 mm with holes of 57.7 mm diameter at the center and 11.1 mm diameter in each corner. The inner piece was 57.2 mm in diameter and 3.2 mm thick with a hole of 12.7 mm at the center. These pieces formed a square butt joint with a 0.25-mm root opening.

The fixture for circular-patch welding is shown in Fig. 1B. The outer piece was sandwiched between a copper plate (152 × 152 × 19 mm) at the bottom and a copper ring (19 mm thick, 83 mm ID, and 152 mm × 152 mm on the outside) at the top. The workpiece, together with the copper plate and the copper ring, were bolted to a stainless steel base plate of 203 x 203 x 25.4 mm. The bolts were tightened with a torque wrench to the same torque of 47.5 m-N to ensure consistent restraint conditions. A similar design was used by Nelson et al. (Ref. 26) for assessing solidification cracking in steel welds.

The workpiece was separated from the copper plate and the copper ring by steel washers 1.6 mm thick, 12.2 mm ID, and 23.5 mm OD. Without the washers, it was difficult to make complete joint-penetration welds because of the heat sink effect of copper.

In addition to the welding wires, 99.999% pure Cu in the form of 1-mm-diameter wire was also used in some experiments. It was placed in a 1 × 1 mm groove of 50.8 mm diameter at the top surface of the inner piece, and gas tungsten arc (GTA) welded with Ar shielding to melt and mix with the surrounding base metal before circular-patch welding. The conditions for GTAW were 16 V, 75 A, DC electrode negative, and 7.4 mm/s welding speed (based on a rotation speed of 2.8 rpm and a 50.8-mm diameter). The resultant weld bead completely penetrated and was about 4 mm wide at the top, well within and thus fully incorporated into the subsequent circular-patch weld. One wire was used in the case of Alloy 7075 and two in 2024, where they were placed in a 1-mm-deep × 2-mm-wide groove of 50.8 mm diameter at the top surface of the inner piece.

Circular-patch welding was conducted using the gas metal arc welding (GMAW) process with electrode-positive polarity (DCEP) and Ar shielding. The inner and outer pieces were not tack welded prior to GMAW. Since the two pieces were held down tightly, there was no distortion during or after welding. The distance between the contact tube and workpiece was about 25.4 mm, and the torch was perpendicular to the workpiece. The welding speed was 4.2 mm/s (based on a 1.6 rpm rotation speed and a 50.8 mm diameter). The welding wire was 1.2 mm in diameter and was positioned at 25.4 mm from the center of the workpiece. The wire feed rate was 93 mm/s, the average current 140 A, and the voltage 22 V. With filler metal 5356, however, the wire feed rate and the voltage were raised to 106 mm/s and 24 V, respectively, in order to raise the average welding current to 125 A. The nominal power (voltage × current) was 3000 W with filler metal 5356, and 3080 W with all others.

The weld surface was cleaned with a solution of 48 vol% HF. Macrographs of the welds were taken with a digital camera. The welds were then sectioned, polished, and etched with 0.5 vol% HF in water. The transverse cross-sectional area of each weld was determined with a digital camera and a computer using commercial software. The weld microstructure was examined with an optical microscope.

Results and Discussion

Weld-Metal Composition

The weld metal composition was assumed uniform in view of the Lorenz force, surface tension gradients, and droplet impingement that help mix the filler metal

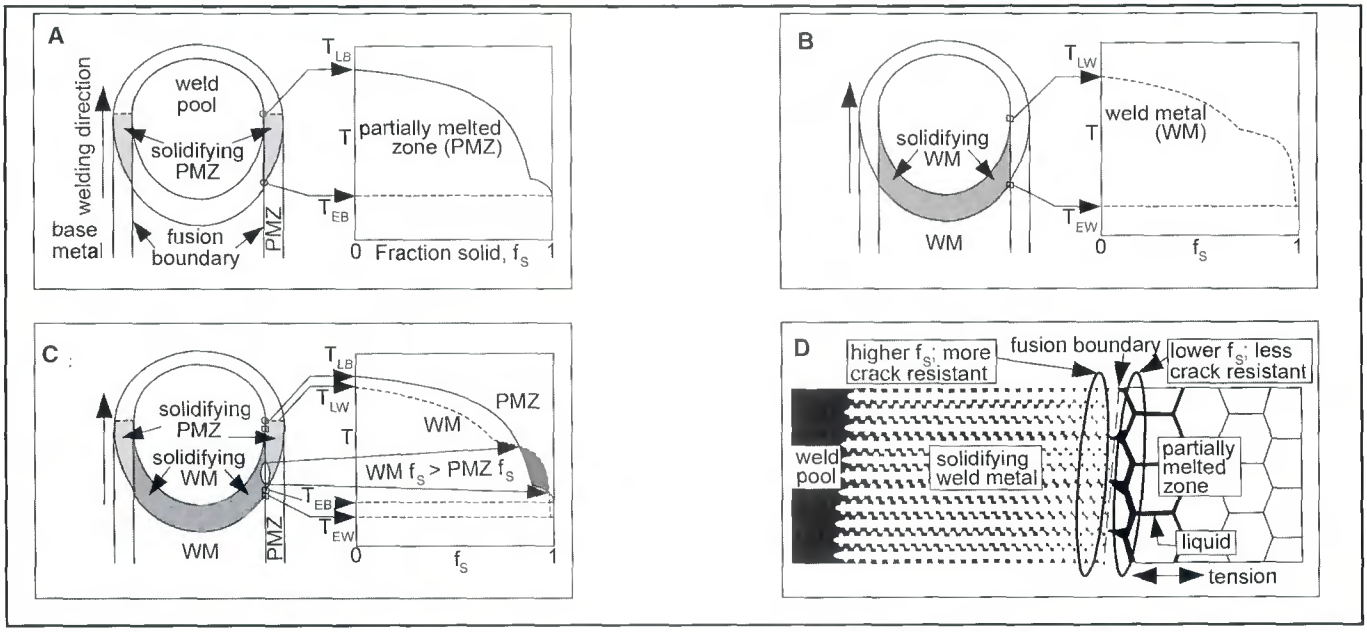

Fig. 3 — T-f_S curves along fusion boundary. A — Solidifying PMZ; B — solidifying WM; C — superimposed to show region of WM f_S > PMZ f_S; D — example microstructure of WM f_S > PMZ f_S.

with the melted base metal (Ref. 1). Houldcroft (Ref. 27) has verified that the composition of a single-pass GMA aluminum weld is essentially uniform.

From the conservation of mass, the concentration of any element E in the weld metal, E_{weld}, can be calculated from those in the base metal, E_{base}, the filler metal, E_{filler}, and the Cu wire, E_{wire}, as follows:

$$E_{weld} = \frac{\left[V_{base}\rho_{base}E_{base} + (V_{weld} - V_{base} - V_{wire}) \rho_{filler}E_{filler} + V_{wire}\rho_{wire}E_{wire}\right]}{(V_{weld}\rho_{weld})} \quad (1)$$

where V_{base}, V_{wire}, and V_{weld} are the volumes of the base metal melted, the Cu wire, and the weld, respectively. ρ_{base}, ρ_{filler}, ρ_{wire}, and ρ_{weld} are the densities of the base metal, the filler metal, the Cu wire, and the weld, respectively. The densities of 7075, 2024, 4145, 5356, and pure Cu are 2.81, 2.78, 2.74, 2.64, and 8.96 g/cm^3, respectively (Ref. 25). The density of the weld ρ_{weld} is taken as the density of the base metal as an approximation. The denominator in Equation 1 represents the total mass of the weld. The 1st, 2nd, and 3rd terms in the numerator, on the other hand, represent the contributions of mass of element E from the melted base metal, the filler metal, and the Cu wire, respectively.

Figure 2 shows the schematic sketch of the weld transverse cross section, which is considered rectangular as an approximation. The volume of the weld is $V_{weld} = \pi h_{weld}[(R_o)^2 - (R_i)^2]$, where R_i is the inner radius, R_o the outer radius, and h_{weld} the height of the rectangle (weld). Likewise, the volume of the base metal melted plus that of the Cu wire is $V_{base} + V_{wire} = \pi h_{base}[(R_o)^2 - (R_i)^2]$, where h_{base} is the thickness of the base metal (workpiece). The volume of the Cu wire is $V_{wire} = (2\pi R_{wire})A_{wire}$, where R_{wire} is the radius of the ring formed by the wire (25.4 mm), and A_{wire} is the cross-sectional area of the wire, that is, $\pi(1\ mm)^2/4$ for a 1-mm-diameter Cu wire. The very tiny space between the Cu wire and the grove was insignificant and thus ignored.

The transverse macrograph of the weld was taken with a digital camera and enlarged on a computer monitor. The cross-sectional area of the entire weld, A_{weld}, and that of the base metal melted plus the wire, $A_{base} + A_{wire}$, were determined using commercial computer software. The inner radius R_i and outer radius R_o of the weld were selected such that the cross-sectional area of the melted base metal $A_{base} + A_{wire} = h_{base}(R_o - R_i)$. The height of the rectangle (weld) h_{weld} was then selected such that $A_{weld} = h_{weld}(R_o - R_i)$.

In the absence of a Cu wire and assuming the same density for all materials, Equation 1 becomes

$$E_{weld} = \frac{V_{base}\rho_{base}E_{base} + (V_{weld} - V_{base})\rho_{filler}E_{filler}}{V_{weld}\rho_{weld}} = \frac{A_{base}E_{base} + (A_{weld} - A_{base})E_{filler}}{A_{weld}} \quad (2)$$

or

$$E_{weld} = E_{base}\frac{A_{base}}{A_{weld}} + E_{filler}\frac{(A_{weld} - A_{base})}{A_{weld}} = E_{base}(Dilution\ Ratio) + E_{filler}(1 - Dilution\ Ratio) \quad (3)$$

Thus, it is shown that without a Cu wire Equation 1 reduces to Equation 3, which is the conventional way of calculating the weld metal composition from the weld transverse macrograph and the compositions of the base metal and the filler metal. The dilution ratio, that is, the extent the welding wire is diluted by the melted base metal, is as follows:

$$Dilution\ Ratio = \frac{V_{base}}{V_{weld}} = \frac{h_{base}(R_o^2 - R_i^2)}{h_{weld}(R_o^2 - R_i^2)} = \frac{h_{base}}{h_{weld}} = \frac{h_{base}(R_o - R_i)}{h_{weld}(R_o - R_i)} = \frac{A_{base}}{A_{weld}} \quad (4)$$

Thus, it is shown that Equation 4 further reduces to the case for a straight weld if the quantity $(R_o - R_i)$ is substituted by the width of the straight weld.

Calculating T-f_S Curves of Weld Metal and PMZ

The curves of temperature (T) vs. solid fraction (f_S) were calculated for both the weld metal (WM) and the PMZ based on

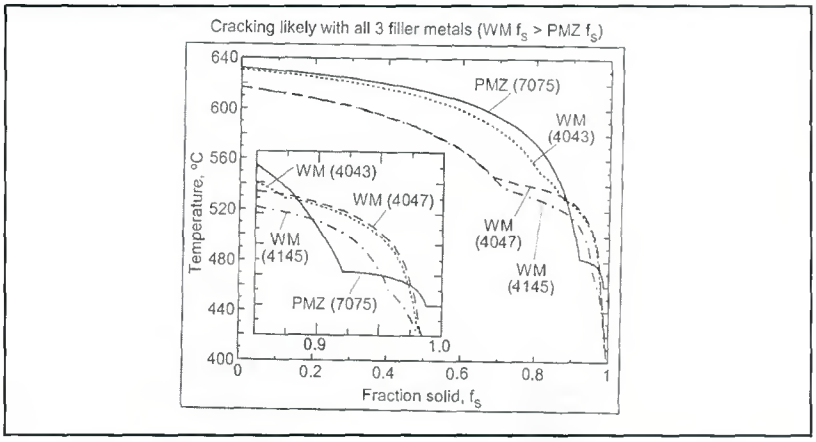

Fig. 4 — T-f_S curves predicting crack susceptibility of 7075 welds made with filler metals 4043, 4047, and 4145 at 65% dilution of filler metal by base metal. Curves calculated using Pandat *software of CompuTherm LLC (Ref. 28).*

the multicomponent Scheil model for alloy solidification. For binary alloys the fraction solid of a semisolid at any temperature during solidification can be calculated by using the simple Scheil equation (Ref. 1), which is based on the following assumptions: complete diffusion in liquid, no diffusion in solid, equilibrium between solid and liquid at the solid-liquid interface, and straight solidus and liquidus lines of the binary phase diagram (that is, the equilibrium partition ratio, k, and the slope of the liquidus line, m_L, are both constant).

For multicomponent alloys, however, the fraction solid needs to be calculated numerically because the simple Scheil equation is for binary alloys only. The computer program *Pandat* (Ref. 28) was used. It is a software package for calculating multicomponent phase diagrams, solidification paths, and thermodynamic properties. PanAluminum (Ref. 29) was also used. It is a thermodynamic database for aluminum alloys based on experimental data of thermodynamic properties and phase equilibria. The software and the database have been tested extensively against binary and multicomponent aluminum alloys. All thermodynamic models are built in *Pandat*, and all model parameters are listed in the database. In the computation of the phase diagram, the compositions of the solid and liquid phases at each temperature are calculated, based on which k and m_L at each temperature are calculated, that is, k and m_L are both temperature dependent. No special equation forms are needed, such as sums of polynomials.

For the present study, the following six components were selected from PanAluminum: Al, Cu, Mg, Mn, Si, and Zn. The actual contents of these elements given in Table 1 were used in the calculation of the fraction solid. The Scheil model for multicomponent alloys was used as an approximation, but with temperature-dependent k and m_L. It was assumed that both the primary and secondary phases would nucleate without significant undercooling. More advanced solidification models can be used to calculate the fraction solid more accurately than the Scheil model.

T-f_S Curves and Susceptibility to Liquation Cracking

The relationship between the T-f_S curves and the susceptibility to liquation cracking is illustrated in Fig. 3. Figure 3A shows the T-f_S curve for a solidifying PMZ along the fusion boundary. For convenience of discussion, the curve is shown side by side with a weld pool. The PMZ has the same (local average) composition as the base metal. The curve begins at the liquidus temperature of the base metal T_{LB} and ends at the eutectic temperature of the base metal T_{EB}. The f_S distribution along the fusion boundary can be determined from the T-f_S curve and the temperature distribution along the fusion boundary. Similarly, Fig. 3B shows the T-f_S curve for a solidifying weld metal (WM), that is, the mushy zone, along the fusion boundary from the liquidus temperature of the weld metal T_{LW} to the eutectic temperature of the weld metal T_{EW}. The two curves are superimposed in Fig. 3C. The region along the weld interface encircled by an oval corresponds to the shaded area between the two T-f_S curves, where the condition of WM f_S > PMZ f_S exists during solidification. As mentioned previously, this region is susceptible to liquation cracking according to the recent studies of Kou et al. (Refs. 20, 21, 23). An example microstructure of WM f_S > PMZ f_S is shown schematically in Fig. 3D. It shows that near the fusion boundary the PMZ is lower in fraction solid and hence resistance to cracking than the weld metal.

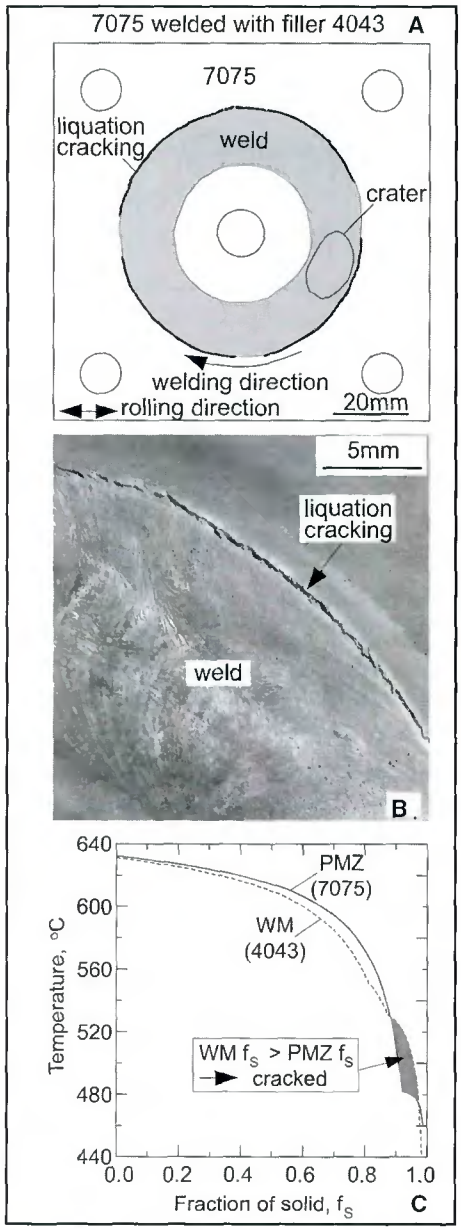

Fig. 5 — Liquation cracking in Alloy 7075 welded with filler metal 4043. A — Overview; B — macrograph; C — T-f_S curves. Crack susceptibility predicted by T-f_S curves confirmed. Curves calculated using Pandat *software of CompuTherm LLC (Ref. 28).*

Experimental data have shown that the strength (Refs. 30–34) of a semisolid aluminum alloy increases with increasing fraction solid (decreasing temperature). Flemings (Ref. 30) has pointed out that the strength of a semisolid is very low until some given fraction of solid is reached, usually in the range of 0.2 to 0.4 (about 0.3). The solidification shrinkage of aluminum is as high as 6.6% (Ref. 30), and the thermal expan-

sion coefficient of aluminum is roughly twice that of iron-base alloys. Therefore, aluminum alloys have a tendency to contract significantly during solidification. During welding the solidifying PMZ is connected to the solidifying weld metal along the fusion boundary and is thus under the tensile strains induced by weld-metal solidification shrinkage and thermal contraction. Consequently, a solidifying PMZ lower in fraction solid and hence crack resistance than the solidifying weld metal is likely to be crack susceptible during solidification, say, after reaching a fraction solid of 0.3 (Ref. 23). Here, the secondary effect of the microstructure and grain size on the strength or crack resistance of a semisolid is neglected as an approximation.

Predicting Crack Susceptibility of 7075 Welds with T-f_S Curves

The dilution of the filler metal by the base metal in butt-joint welds ranges from about 40% for V-groove joints to about 80% for square groove joints (Ref. 2). For the welds in square groove joints in the circular-patch test used in our recent studies (Refs. 20, 21, 23), the dilution ratio was about 65%. Thus, for the purpose of discussion, a 65% dilution will be used in the present study.

Figure 4 shows the T-f_S curves calculated for Alloy 7075 welds made with three different filler metals at 65% dilution, that is, filler metals 4043 (essentially Al-5Si), 4047 (essentially Al-12Si), and 4145 (essentially Al-4Cu-10Si). With 4043, WM f_S > PMZ f_S occurs during PMZ terminal solidification. With 4047, the situation is similar though the fraction solid is significantly lower than that with 4043 at higher temperatures. With 4145, the fraction solid is close to that with 4047 at higher temperatures but becomes lower than that with 4047 before PMZ terminal solidification. However, WM f_S > PMZ f_S still occurs during solidification. Consequently, all these three welds are susceptible to liquation cracking.

Confirming Crack Susceptibility of 7075 Welds

For convenience, all welds are identified by two numbers — the first referring to the workpiece and the second the filler metal. For instance, weld 7075/4043 refers to the weld made in Alloy 7075 with filler metal 4043. The experimental results are summarized in Table 2. All cracks in the PMZ were intergranular, typical of liquation cracking. Liquation cracking occurred along the outer edge of the weld but not the inner edge. In principle, the shrinkage of a circular weld in a square workpiece restrained at four sides can induce tension at the outer edge and compression at the inner edge.

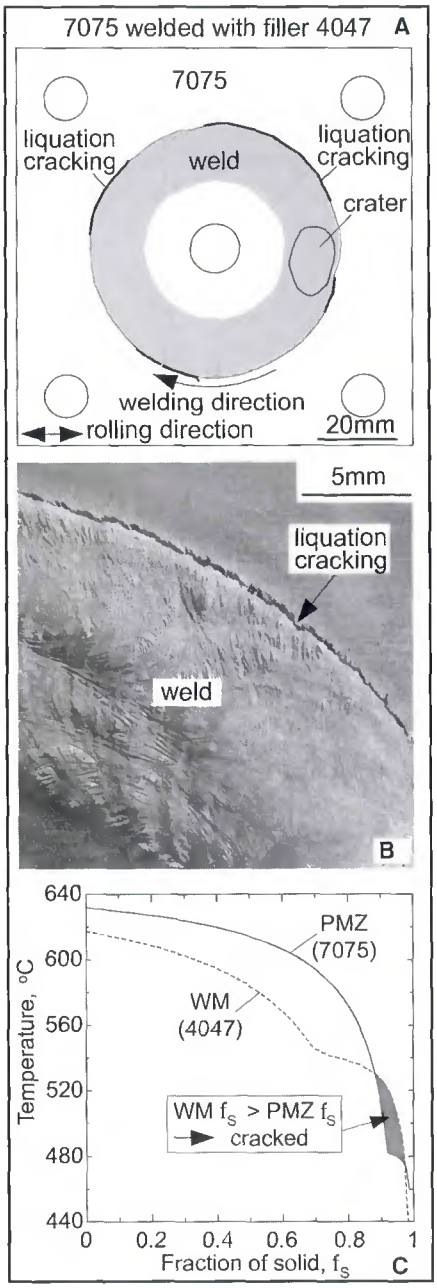

Fig. 6 — Liquation cracking in Alloy 7075 welded with filler metal 4047. A — Overview; B — macrograph; C — T-f_S curves. Crack susceptibility predicted by T-f_S curves confirmed. Curves calculated using Pandat *of CompuTherm LLC (Ref. 28).*

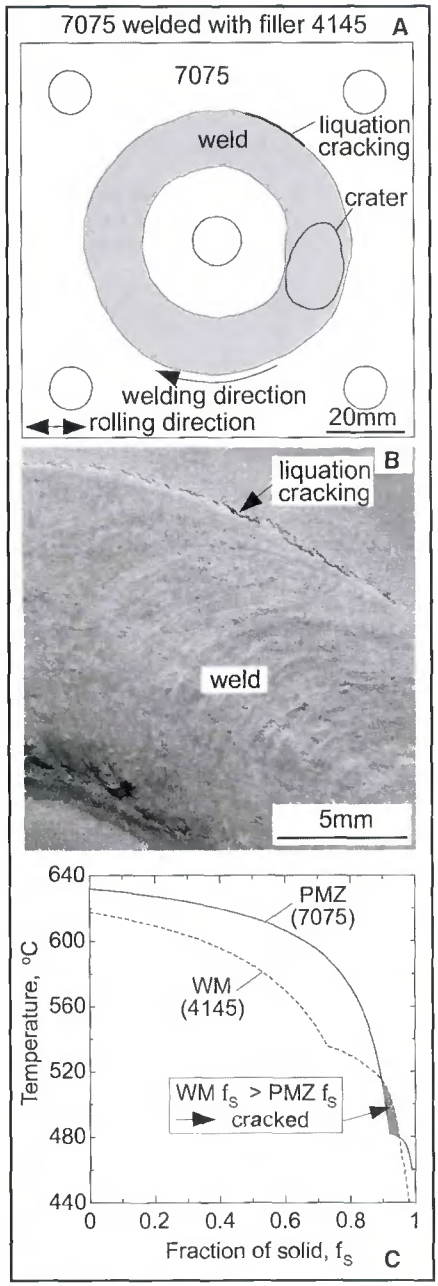

Fig. 7 — Liquation cracking in Alloy 7075 welded with filler metal 4145. A — Overview; B — macrograph; C — T-f_S curves. Crack susceptibility predicted by T-f_S curves confirmed. Curves calculated using Pandat *of CompuTherm LLC (Ref. 28).*

This suggests liquation cracking along the outer edge of the weld but not the inner one. It also suggests the existence of tensile stresses in the circumferential direction to induce transverse cracks. However, it is not clear why such cracks were observed in only one weld (weld 2024/1100). Perhaps other factors could also have played a significant role, such as the extent of WM f_S > PMZ f_S (the temperature range and the f_S difference, which are greatest in weld 2024/1100) and the uneven heat distribution in the circular weld.

Weld 7075/4043 had a dilution ratio of 65.5%, as shown in Table 2. Based on the dilution ratio and the compositions of the base metal and the welding wire, the weld-metal composition was Al-0.95Cu-1.70Mg-0.033Mn-1.86Si-3.78Zn. Figure 5A is the overview of the weld traced from its digital photograph with the help of computer software. The cracks were marked with thick

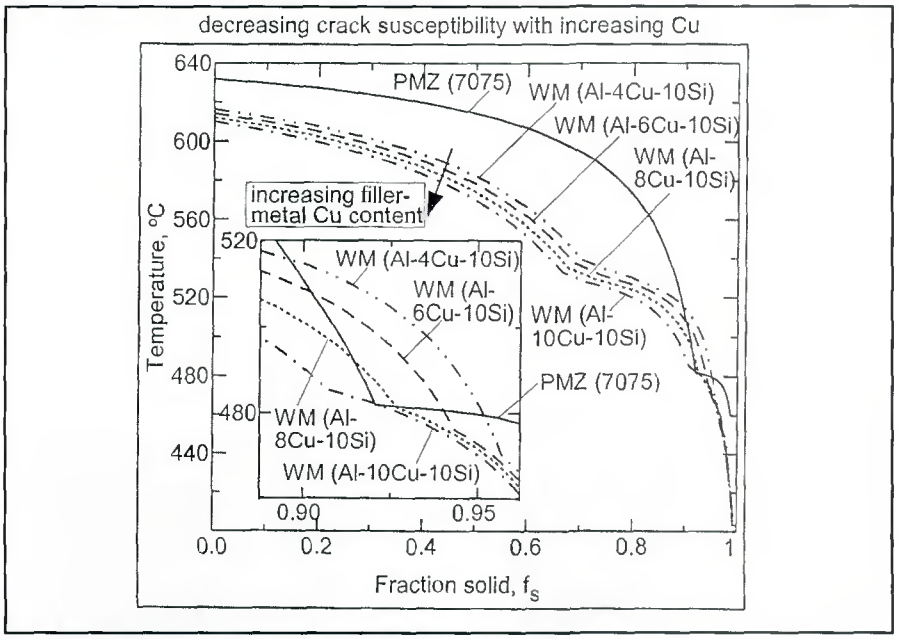

Fig. 8 — T-f_S curves predicting reduction of liquation-cracking susceptibility of 7075 welds by increasing Cu content in filler metal Al-xCu-10Si to minimize extent of WM f_S > PMZ f_S during solidification, 65% dilution. Curves calculated using Pandat *software of CompuTherm LLC (Ref. 28).*

lines for clarity. Such an overview was used instead of the photograph itself because cracks would be too small to see at the magnification of the overview.

Liquation cracking, shown in Fig. 5B, was severe, extending along 76% of the weld length, as shown in Table 2. Figure 5C, based on 65.5% dilution, shows that WM f_S > PMZ f_S exists during solidification as expected.

As shown in Table 2, weld 7075/4047 had a dilution ratio of 65.9% and a composition of Al-0.97Cu-1.71Mg-0.033Mn-4.01Si-3.82Zn. Figure 6A shows the overview of the top of the weld. Liquation cracking occurred, extending along 42% of the weld length, as shown in Fig. 6A and B and Table 2. This liquation cracking is less severe than that in weld 7075/4043 (76%). Figure 6C, based on 65.9% dilution, shows that WM f_S > PMZ f_S during solidification as expected.

Weld 7075/4145 had a dilution ratio of 67.7% and a composition of Al-2.24Cu-1.77Mg-0.037Mn-3.25Si-3.94Zn. Liquation cracking still occurred, but extending along only 8% of the weld length, as shown in Fig. 7A and B and Table 2. This liquation cracking is much less severe than that in welds 7075/4043 (76%) and 7075/4047 (42%). Figure 7C, based on 67.7% dilution, shows that WM f_S > PMZ f_S during solidification as expected.

Table 2 — Summary of Experimental Results

Weld	Dilution ratio	Weld metal composition (wt-%)	Liquation crack length (cm)	Crack length/ weld length*
2024/1100	63.4%	Al-2.95Cu-0.95Mg-0.40Mn-0.067Si-0.083Zn	5.55	26%
2024/4043	68.8%	Al-3.16Cu-1.t0Mg-0.43Mn-1.68Si-0.06Zn	<1.0	<6%
2024/5356+Cu	NA	Al-14.27Cu-2.51Mg-0.43Mn-0.12Si-0.11Zn	0	0
7075/4043	65.5%	Al-0.95Cu-1.70Mg-0.033Mn-1.86Si-3.78Zn	14.36	76%
7075/4047	65.9%	Al-0.97Cu-1.71Mg-0.033Mn-4.01Si-3.82Zn	7.75	42%
7075/4145	67.7%	Al-2.24Cu-1.77Mg-0.037Mn-3.25Si-3.94Zn	1.57	8%
7075/4145+Cu	NA	Al-6.34Cu-1.81Mg-0.038Mn-2.96Si-4.03Zn	0	0

* Weld length = (length of weld outer edge + length of weld inner edge)/2

Reducing Crack Susceptibility of 7075 Welds with Help of T-f_S Curves

Figure 4 shows that the extent of WM f_S > PMZ f_S during solidification is not reduced when the Si contents of the filler metal and hence the weld metal are increased by switching from filler metal 4043 (essentially Al-5Si) to 4047 (essentially Al-12Si). In contrast, it is reduced when the Cu contents of the filler metal and hence the weld metal are increased by switching from filler metal 4047 (essentially Al-12Si) to 4145 (essentially Al-4Cu-10Si).

Figure 8 shows at 65% dilution the effect of increasing Cu content on the extent of WM f_S > PMZ f_S during solidification. The filler metals Al-xCu-10Si all have 10% Si as in 4145 (essentially Al-4Cu-10Si), but the Cu content is increased from 4% (in filler metal Al-4Cu-10Si) to 10% (in filler metal Al-10Cu-10Si). As shown, the extent of WM f_S > PMZ f_S during solidification is reduced as the filler metal Cu content increases. The weld metal Cu content increases from 2.34% with filler metal Al-4Cu-10Si to 4.44% with filler metal Al-10Cu-10Si.

To confirm the effect of increasing Cu content on reducing the crack susceptibility of 7075 welds without going through the highly costly process of producing special filler wires from casting, heat treating, swaging, and drawing, a 1-mm-diameter pure Cu wire was preplaced and mixed with the base metal by GTAW before circular-patch welding with filler metal 4145, as already described in the experimental procedure.

The composition of weld 7075/4145+Cu, determined from the weld transverse macrograph, Equation 1, and the compositions and densities of the materials involved, was Al-6.34Cu-1.81Mg-0.038Mn-2.96Si-4.03Zn. As shown in Fig. 9A, liquation cracking was eliminated, thus confirming the predicted effect of increasing Cu content on reducing the crack susceptibility. Figure 9B, a micrograph parallel to and near the workpiece top surface, shows no evidence of liquation cracking. As shown in Fig. 9C, the desirable condition of WM f_S < PMZ f_S was maintained throughout solidification, which explains the absence of liquation cracking.

The composition of a filler metal needed to produce a weld with 6.34% Cu at 65% di-

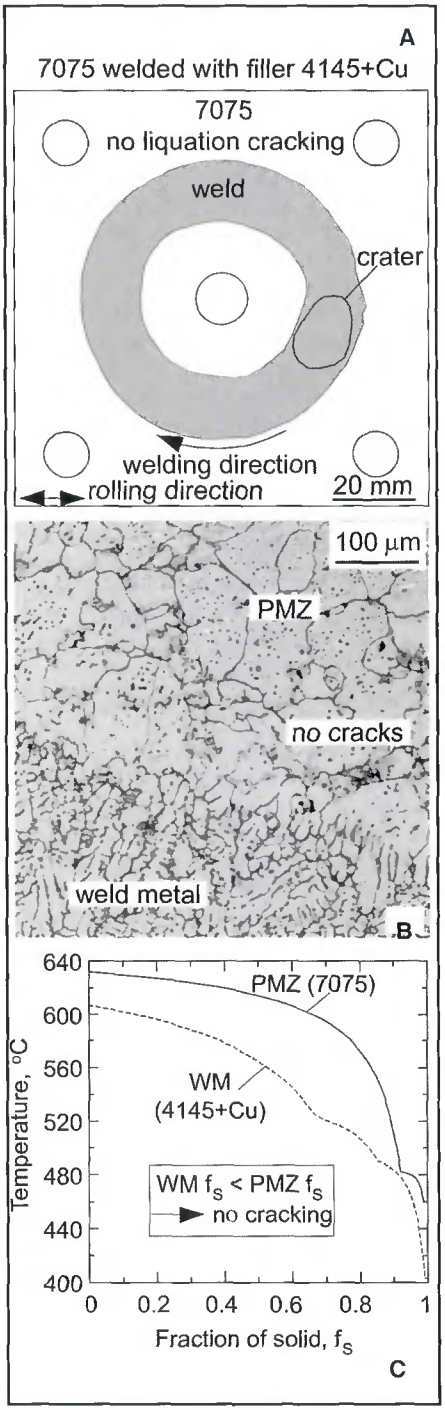

Fig. 9 — Alloy 7075 welded with filler metal 4145 plus extra Cu. A — Overview; B — micrograph; C — T-f_S curves. Elimination of cracking confirms effect of increasing filler-metal Cu content on reducing crack susceptibility predicted by T-f_S curves. Curves calculated using Pandat *software of CompuTherm LLC (Ref. 28).*

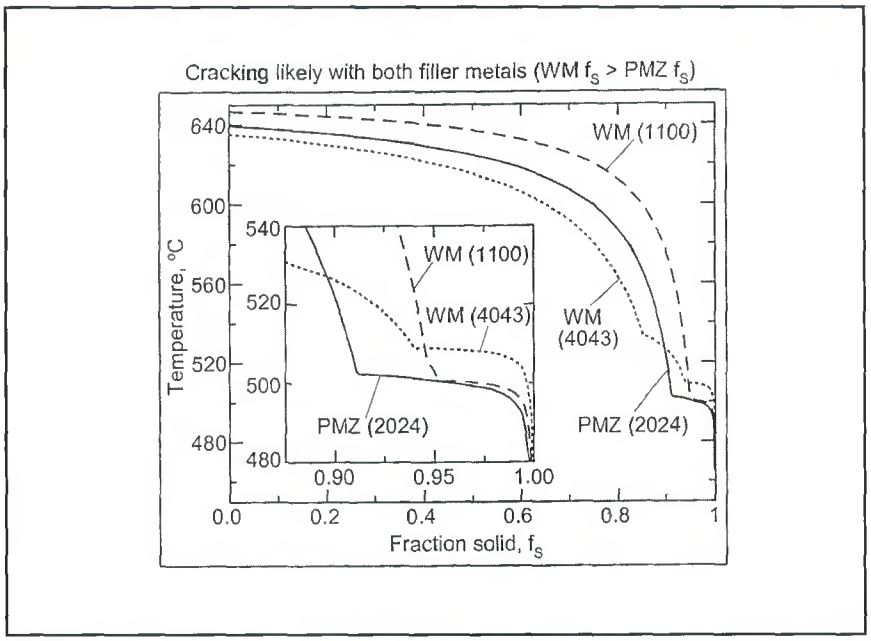

Fig. 10 — T-f_S curves predicting crack susceptibility of 2024 welds made with filler metals 1100 and 4043 at 65% dilution of filler metal by base metal. Curves calculated using Pandat *software of CompuTherm LLC (Ref. 28).*

lution is approximately Al-15Cu-8Si. In reality, the Cu content of the filler metal can be less than 15% as the experiment was meant only to demonstrate, not optimize, the effect of the Cu content on liquation cracking. A WM T-f_S curve touching or even slightly cutting the PMZ T-f_S curve is likely to be all right.

Predicting Crack Susceptibility of 2024 Welds with T-f_S Curves

Figure 10 shows the T-f_S curves calculated for Alloy 2024 welds made with two different filler metals at 65% dilution, that is, filler metals 1100 (essentially pure Al) and 4043 (essentially Al-5Si). With 1100, WM f_S > PMZ f_S exists throughout PMZ solidification, and with 4043 it occurs during PMZ terminal solidification. Consequently, both welds are susceptible to liquation cracking.

Confirming Crack Susceptibility of 2024 Welds

Weld 2024/1100 had a dilution ratio of 63.4% and a composition of Al-2.95Cu-0.95Mg-0.40Mn-0.067Si-0.083Zn. Liquation cracking occurred, extending along 26% of the weld length, as shown in Fig. 11A and B and Table 2. Some transverse cracks were observed in the PMZ in the upper-left region of the weld, as shown in Fig. 11A. As mentioned previously, these cracks might have been induced by tensile stresses in the circumferential direction of the weld outer edge. Figure 11C, based on 63.4% dilution, shows that WM f_S > PMZ f_S throughout solidification including f_S > 0.3 as indicated by the shaded area. However, although WM f_S > PMZ f_S existed throughout solidification, liquation cracking extended along only 26% of the weld length. This is probably because Alloy 2024, which is less heavily alloyed than Alloy 7075, tends to liquate less severely than Alloy 7075 (Ref. 22). Furthermore, weld 2024/1100 was in a composition range that is rather susceptible to solidification cracking (Ref. 35), as evident from the severe solidification cracking shown in Fig. 11. Thus, solidification cracking, once it started, probably relaxed the tensile strains in the PMZ nearby and caused liquation cracking to stop (Ref. 20).

Weld 2024/4043 had a dilution ratio of 68.8% and a composition of Al-3.16Cu-1.10Mg-0.43Mn-1.68Si-0.062Zn. No liquation cracking was visible even under a magnifier, as shown in Fig. 12A. However, the micrograph parallel and near the workpiece surface shown in Fig. 12B still revealed liquation cracking in the PMZ. The micro cracks are intergranular, typical of liquation cracking. Figure 12C, based on 68.8% dilution, shows that WM f_S > PMZ f_S during terminal solidification as expected.

Reducing Crack Susceptibility of 2024 Welds with Help of T-f_S Curves

Figure 13 shows at 65% dilution the effect of increasing Cu content on the extent

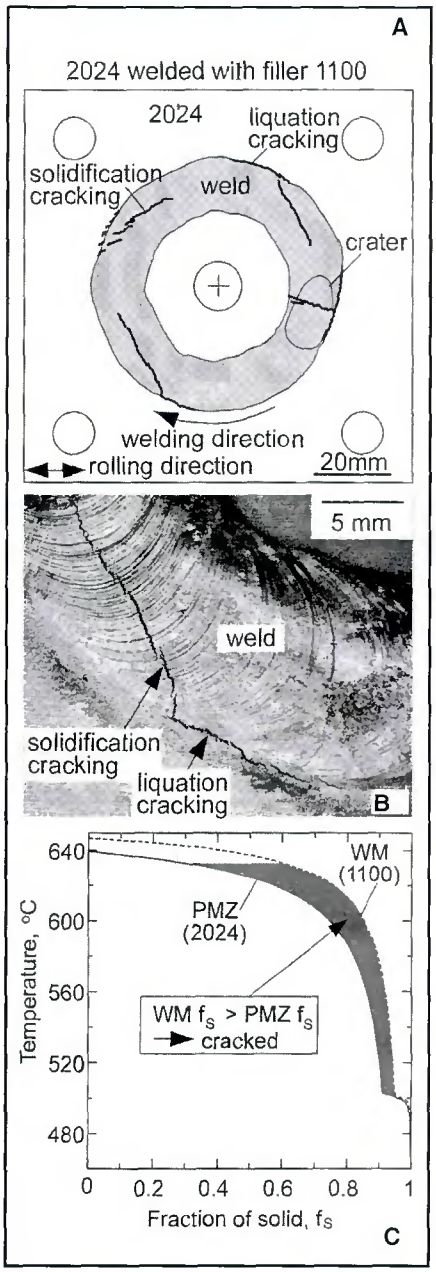

Fig. 11 — Liquation cracking in Alloy 2024 welded with filler metal 1100. A — Overview; B — macrograph; C — T-f_S curves. Crack susceptibility predicted by T-f_S curves confirmed. Curves calculated using Pandat of CompuTherm LLC (Ref. 28).

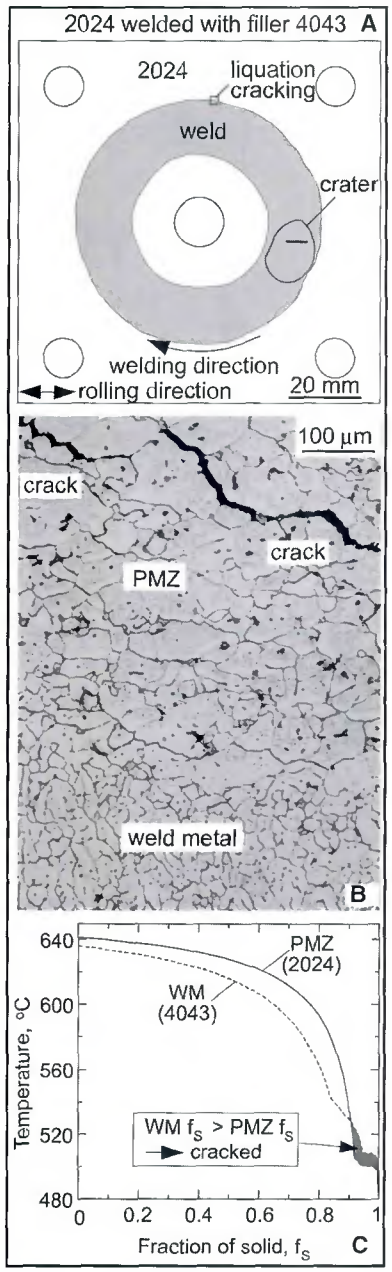

Fig. 12 — Liquation cracking in Alloy 2024 welded with filler metal 4043. A — Overview; B — micrograph; C — T-f_S curves. Crack susceptibility predicted by T-f_S curves confirmed. Curves calculated using Pandat *software of CompuTherm LLC (Ref. 28).*

of WM f_S > PMZ f_S during solidification. The filler metals Al-5Mg-xCu all have 5% Mg as in filler metal 5356 (essentially Al-5Mg), but the Cu content is increased from 0% (in filler metal Al-5Mg) to 20% (in filler metal Al-5Mg-20Cu). Filler metals other than 5356 can also be selected. However, since 4145 has already been chosen in the case of Alloy 7075, a different filler metal, that is, 5356 was selected for Alloy 2024. Furthermore, the alloying element to be varied in content does not have to be Cu again as long as the crack susceptibility can be effectively reduced. However, Cu was chosen here again because it is readily available in the wire form with high purity. As shown in Fig. 13, the extent of WM f_S > PMZ f_S during solidification is reduced as the filler metal Cu content increases. The weld metal Cu content increases from 2.99% with filler metal Al-5Mg to 9.99% with filler Al-5Mg-20Cu.

To confirm the effect of increasing Cu content on reducing the crack susceptibility of 2024 welds, two 1-mm-diameter pure Cu wires were preplaced and mixed with the base metal by GTAW before circular-patch welding with filler metal 5356, as already described in the experimental procedure.

The composition of weld 2024/5356+Cu, determined from the weld transverse macrograph, Equation 1, and the compositions and densities of the materials involved, was Al-14.27Cu-2.51Mg-0.43Mn-0.12Si-0.11Zn. As shown in Fig. 14A, liquation cracking was eliminated, thus confirming the predicted effect of increasing Cu content on reducing the crack susceptibility. Figure 14B, a micrograph on the transverse cross-section of the weld, shows no evidence of liquation cracking. As shown in Fig. 14C, the desirable condition of WM f_S < PMZ f_S was maintained throughout solidification, which explains the absence of liquation cracking.

Had only one Cu wire been used instead of two, the weld metal would have contained 8.72% Cu, which is below the aforementioned 9.99% Cu in a weld made with filler metal Al-5Mg-20Cu. Therefore, in order to make the Cu content no less than 9.99%, two Cu wires were used. At 65% dilution, the 14.25% Cu in weld 2024/5356+Cu corresponds to a welding wire of essentially Al-4Mg-32Cu. Again, in reality, the Cu content of the filler metal can be significantly less than 32% as the experiment was not meant to optimize the Cu content of the filler metal. In fact, the enlarged portion in Fig. 13 shows that the T-f_S curve of the weld metal made with filler metal Al-5Mg-11Cu nearly coincides with the lower bound of the PMZ T-f_S curve, thus suggesting that a filler metal with a much lower Cu content than 32% is likely to work just as well.

Further Discussion on Cracking

It should be pointed out that T-f_S curves predict crack-susceptible weld compositions, which is a necessary, not sufficient, condition for liquation cracking. For cracking to actually occur, the following additional conditions are also required (Refs. 20, 21): 1) a significant tendency for the workpiece to contract during solidification (such as in the case of aluminum alloys); 2) significant restraint to keep the workpiece from contracting freely (such as in a tightly clamped workpiece); 3) significant liquation to weaken the PMZ (such as in high-strength aluminum alloys or under high heat inputs or both); and 4) no solidification cracking nearby to relax the strains in the PMZ (such as in welds without compositions highly susceptible to solidification cracking) (Ref. 20).

It should also be pointed out that the opposite condition, WM f_S < PMZ f_S does not necessarily imply cracking in the weld metal. The grain-boundary liquid in the PMZ is negligible in quantity as compared

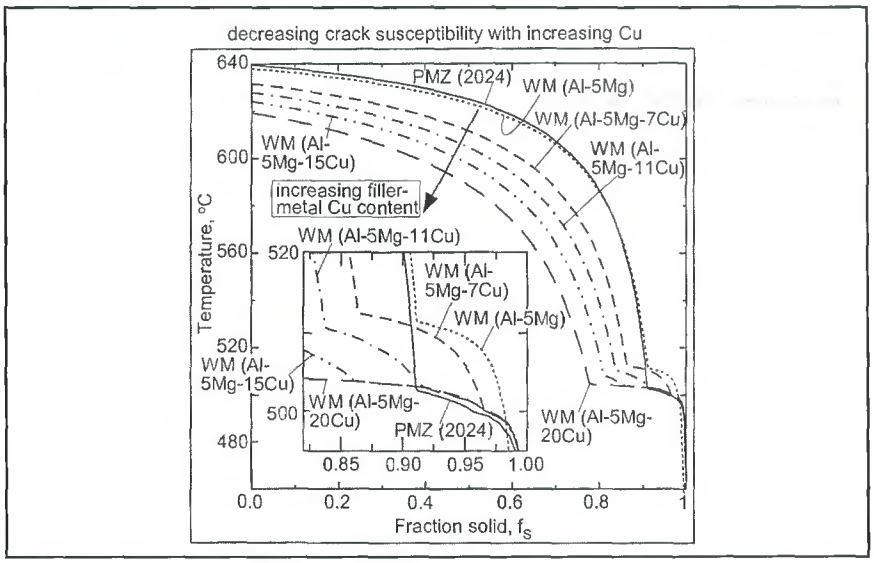

Fig. 13 — T-f_S curves predicting reduction of liquation-cracking susceptibility of 2024 welds by increasing Cu content in filler metal Al-5Mg-xCu to minimize the extent of WM f_S > PMZ f_S during solidification, 65% dilution. Curves calculated using Pandat *software of CompuTherm LLC (Ref. 28).*

to the liquid in the weld pool because the PMZ is much narrower than the weld pool and because the PMZ is only partially melted, as can be seen in Fig. 3D. This suggests that tension induced by PMZ solidification shrinkage is negligible as compared to that induced by weld pool solidification and thus will not promote weld metal cracking when WM f_S < PMZ f_S. If the weld metal composition happens to be in the range of high solidification cracking, for instance, around 3%Cu in Al-Cu alloys and 0.7% Si in Al-Si alloys (Ref. 1), cracking can occur in the weld metal. Otherwise, solidification cracking will not occur in the weld metal even when WM f_S < PMZ f_S.

Finally, it is worth mentioning that the prediction of liquation cracking is usually reliable when the maximum f_S difference between the PMZ and WM T-f_S curves is about 0.05 or above during terminal solidification but less reliable down to about 0.03 (such as the case shown in Fig. 7) or less. Here, the use of the exact compositions of the workpiece and the filler metal is essential as the nominal compositions may vary within the specification ranges. A solidification model more advanced than the Scheil model may also help. However, knowing the exact dilution ratio can be even more important because the dilution ratio can have a rather significant effect on the weld metal composition. Generally speaking, however, for highly crack-susceptible materials such as high-strength aluminum Alloys 7075 and 2024, even a slightly higher fraction solid of the weld metal than the PMZ can cause liquation cracking. This is because these materials are highly susceptible to liquation and the PMZ can thus be severely weakened and become highly susceptible to cracking.

Conclusions

Based on the curves of temperature vs. fraction solid (T-f_S) of the weld metal (WM) and the partially melted zone (PMZ), the recent discovery of the harmful solidification condition of WM f_S > PMZ f_S in welds susceptible to liquation cracking was applied in the present study to both predict and reduce the liquation-cracking susceptibility of complete joint penetration aluminum welds. T-f_S curves were calculated based on the multicomponent Scheil solidification model for two highly crack-susceptible alloys, 7075 and 2024, to predict the crack susceptibility of their welds made with various filler metals and to reduce it by adjusting the filler metal composition. These predictions were tested in circular-patch welding.

The conclusions are as follows:

1. T-f_S curves predict that welds of Alloy 7075 made with filler metals 4043, 4047, and 4145 at 65% dilution, a level typical in butt joint welding (including circular-patch welding) of aluminum alloys, are susceptible to liquation cracking.

2. Circular-patch welding of Alloy 7075 with filler metals 4043, 4047, and 4145 has confirmed the crack susceptibility predicted by the T-f_S curves. Liquation cracking has been observed in all these welds.

3. The severity of liquation cracking in these 7075 welds is highest with filler metal 4043 and lowest with 4145, which has the lowest extent of WM f_S > PMZ f_S during solidification.

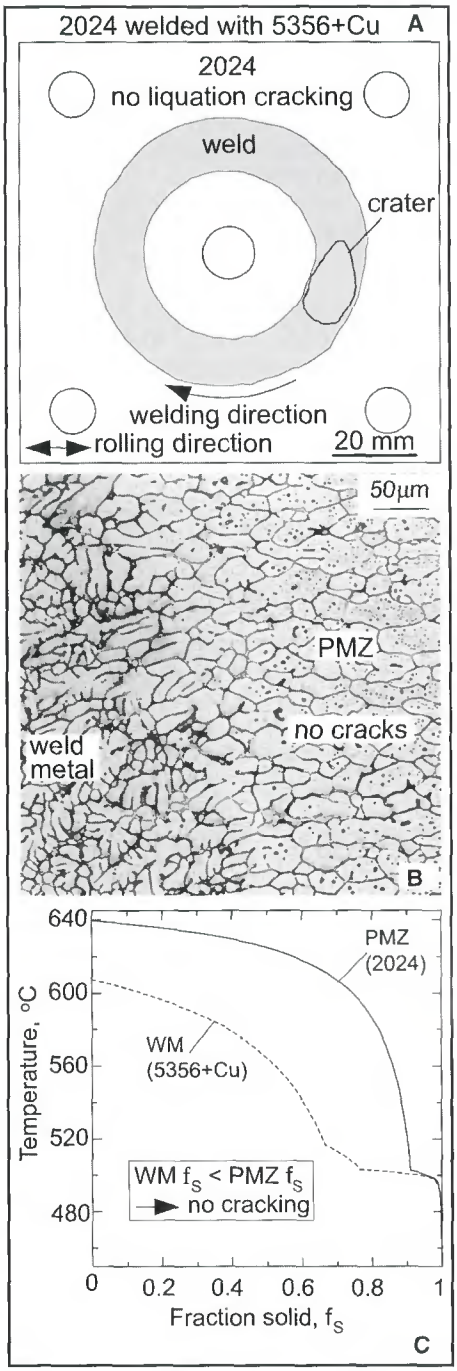

Fig. 14 — Alloy 2024 welded with filler metal 5356 plus extra Cu. A — Overview; B — transverse micrograph; C — T-f_S curves. Elimination of cracking confirms effect of increasing filler-metal Cu content on reducing crack susceptibility predicted by T-f_S curves. Curves calculated using Pandat software *of CompuTherm LLC (Ref. 28).*

4. T-f_S curves suggest that increasing the weld-metal Cu, not Si, content of 7075 welds can effectively reduce the extent of WM f_S > PMZ f_S during solidification and thus the crack susceptibility.

5. T-f_S curves predict that if the Cu content in filler metal Al-4Cu-10Si (which is essentially 4145) is increased, the extent of

WM f_S > PMZ f_S during solidification and hence the crack susceptibility of 7075 welds will decrease.

6. Circular-patch welding of Alloy 7075 with filler metal 4145 plus extra Cu has confirmed elimination of liquation cracking as predicted by the T-f_S curves.

7. T-f_S curves predict that welds of Alloy 2024 made with filler metals 1100 and 4043 at 65% dilution are susceptible to liquation cracking.

8. Circular-patch welding of Alloy 2024 with filler metals 1100 and 4043 has confirmed the crack susceptibility predicted by the T-f_S curves.

9. The severity of liquation cracking in these 2024 welds is much lower with filler metal 4043, which has a much narrower temperature range in which the condition of WM f_S > PMZ f_S exists during solidification.

10. T-f_S curves show that if the Cu content in filler metal Al-5Mg (which is essentially 5356) is increased, the extent of WM f_S > PMZ f_S during solidification and hence the crack susceptibility of 2024 welds will decrease.

11. Circular-patch welding of Alloy 2024 with filler metal 5356 plus extra Cu has confirmed elimination of liquation cracking as predicted by the T-f_S curves.

12. The present study has demonstrated that T-f_S curves can predict the liquation-cracking susceptibility of complete joint-penetration aluminum welds and guide the selection or development of filler metals to minimize the susceptibility by minimizing the extent of WM f_S > PMZ f_S during solidification. With the help of these curves, the filler-metal composition can be adjusted to keep WM f_S < PMZ f_S during solidification to reduce or eliminate the crack susceptibility.

Acknowledgments

This work was supported by National Science Foundation under Grant Nos. DMR-0098776 and DMR-0309468. The authors would like to thank Professor Y. A. Chang of University of Wisconsin-Madison for letting them use the database required for calculating the T-f_S curves. They are grateful to Bruce Albrecht and Todd Holverson of Miller Electric Manufacturing Co., Appleton, Wis., for donating the welding equipment (including Invision 456P power source, and XR-M wire feeder and gun). Some results related to Alloy 2024 were from the unpublished work of Kou and Huang.

References

1. Kou, S. 2003. *Welding Metallurgy, 2nd edition*. pp. 103–114, 151, 272, and 303–339. New York, N. Y., John Wiley and Sons.

2. Dudas, J. H., and Collins, F. R. 1966. Preventing weld cracks in high-strength aluminum alloys. *Welding Journal* 45(6): 241-s to 249-s.

3. Metzger, G. E. 1967. Some mechanical properties of welds in 6061 aluminum alloy sheet. *Welding Journal* 46(10): 457-s to 469-s.

4. Steenbergen, J. E., and Thornton, H. R. 1970. Quantitative determination of the conditions for hot cracking during welding for aluminum alloys. *Welding Journal* 49(2): 61-s to 68-s.

5. Gittos, N. F., and Scott, M. H. 1981. Heat-affected zone cracking of Al-Mg-Si alloys. *Welding Journal* 60(6): pp. 95-s to 103-s.

6. Ma, T., and Den Ouden, G. 1999. Liquation cracking susceptibility of Al-Zn-Mg alloys. *International Journal for the Joining of Materials (Denmark)* 11(3): 61-67.

7. Katoh, M., and Kerr, H. W. 1987. Investigation of heat-affected zone cracking of GTA welds of Al-Mg-Si alloys using the Varestraint test. *Welding Journal* 66(12): 360-s to 368-s.

8. Kerr, H. W., and Katoh, M. 1987. Investigation of heat-affected zone cracking of GMA welds of Al-Mg-Si alloys using the Varestraint test. *Welding Journal* 66(9): 251-s to 259-s.

9. Miyazaki, M., Nishio, K., Katoh, M., Mukae, S., and Kerr, H. W. 1990. Quantitative investigation of heat-affected zone cracking in aluminum alloy 6061. *Welding Journal* 69(9): 362-s to 371-s.

10. Gitter, R., Maier, J., Muller, W., and Schwellinger, P. 1992. Formation and effect of grain boundary openings in AlMgSi alloys caused by welding. *Proceedings of 5th International Conference on Aluminum Weldments*. P. 4.1.1. Editor: Kosteas, D., Ondra, R., and Ostermann, F. Technische Universita Munich, Munchen, Germany.

11. Powell, G. L. F., Baughn, K., Ahmed, N., Dalton, J. W., and Robinson, P. 1995. The cracking of 6000 series aluminum alloys during welding. *Proceedings of International Conference on Materials in Welding and Joining*. Institute of Metals and Materials Australasia, Parkville, Victoria, Australia.

12. Ellis, M. B. D., Gittos, M. F., and Hadley, I. 1997. Significance of liquation cracks in thick section Al-Mg-Si alloy plate. *The Welding Institute Journal (UK)* 6(2): 213–255.

13. Schillinger, D. E., Betz, I. G., Hussey, F. W., and Markus, H. 1963. Improving weld strength in 2000 series aluminum alloys. *Welding Journal* 42: 269-s to 275-s.

14. Young, J. G. 1968. BWRA experience in the welding of aluminum-zinc-magnesium alloys. *Welding Journal* 47(10): 451-s to 461-s.

15. Lippold, J. C., Nippes, E. F., and Savage, W. F. 1977. An investigation of hot cracking in 5083-O aluminum alloy weldments. *Welding Journal* 56(6): 171-s to 178-s.

16. Gutscher, D., and Cross, C. E. 2003. Effect of Cu and Fe on weldability of aluminum 2519. In *Trends in Welding Research*, ASM International, Materials Park, Ohio, pp. 638–641.

17. Huang, C., Kou, S., and Purins, J. R. 2001. Liquation, solidification, segregation and hot cracking in the partially melted zone of Al-4.5Cu welds. *Proceedings of Merton C. Flemings Symposium on Solidification Processing*. pp. 229–234. Edited by Abbaschian, R., Brody, H., and Mortensen, A. The Mineral, Metals and Materials Society, Warrendale, Pa.

18. Kou, S. 2003. Solidification and liquation cracking issues in welding. JOM, June, pp. 37–42.

19. Huang, C., and Kou, S. 2003. Liquation cracking in partial-penetration aluminum welds: Effect of penetration oscillation and backfilling. *Welding Journal* 82(7): 184s–194s.

20. Huang, C., and Kou, S. 2004. Liquation cracking in full-penetration Al-Cu Welds. *Welding Journal* 83(2): 50s–58s.

21. Huang, C., and Kou, S. 2004. Liquation cracking in full-penetration Al-Mg-Si welds. *Welding Journal* 83(4): 111s–122s.

22. Huang, C., Cao, G., and Kou, S. 2004. Liquation cracking in partial-penetration aluminum welds: Assessing tendencies to liquate, crack and backfill. *Science and Technology of Welding and Joining*, vol. 9, pp. 1–9.

23. Cao, G., and and Kou, S. 2005. Liquation cracking in full-penetration Al-Si welds. *Welding Journal* 84(4): pp. 63s–71s.

24. Borland, J. C., and Rogerson, J. H. 1963. Examination of the patch test for assessing hot cracking tendencies of weld metal. *British Welding Journal* 8: 494-499.

25. The Aluminum Association. 1982. *Aluminum Standards and Data*. p. 15 and p. 42, Washington, D.C., The Aluminum Association.

26. Nelson, T. W., Lippold, J. C., Lin, W., and Baselack III, W. A. 1997. Evaluation of the circular patch test for assessing weld solidification cracking, I. Development of a test method. *Welding Journal* 76(3): 110-s to 119-s.

27. Houldcroft, R. T. 1954. Dilution and uniformity in aluminum alloy weld beads. *British Welding Journal* 1: 468 to 472.

28. *Pandat* – Phase diagram calculation software package for multicomponent systems, CompuTherm LLC, Madison, Wis., 53719, 2001.

29. *PanAluminium* – Thermodynamic database for commercial aluminum alloys, CompuTherm LLC, Madison, Wis., 53719, 2001.

30. Flemings, M. C. 1974. *Solidification Processing*. pp. 34–36, pp. 160–162, pp. 256–258, and Appendix B. New York, N. Y., McGraw-Hill.

31. Singer, A. R. E., and Cottrell, S. A. 1946. Properties of the Al-Si alloys at temperatures in the region of the solidus. *Journal of Institute of Metals* 73: 33–54.

32. Pumphrey, W. I., and Jennings, P. H. 1948. High-temperature tensile properties of cast aluminum-silicon alloys and their constitutional significance. *Journal of Institutive of Metals* 74: 203–233.

33. Dahle, K., and Arnberg, L. 1997. Development of strength in solidifying aluminum alloys. *Acta Materialia* 45: 547–559.

34. Arnberg, L., Chaii, G., and Backerud, L. 1993. Determination of dendritic coherency in solidifying melts by rheological measurements. Materials Science and Engineering A173: 101–103.

35. Pumphrey, W. I., and Lyons, J. V. 1948. Cracking during the casting and welding of the more common binary aluminum alloys. *Journal of Institute of Metals* 74: 439–455.